

Ammoniacal Synthesis of Lanthanum Aryloxy Complexes and Observation of a Unique Interconversion between Oxygen- and η^6 -Arene-Bridged Dimeric Species. X-ray Crystal Structures of $\text{La}_2(\text{OAr})_6(\text{NH}_3)_n$ ($n = 0, 2$), $\text{La}(\text{OAr})_3(\text{NH}_3)_4$, and $\text{La}(\text{OAr})_3(\text{THF})_2$ ($\text{Ar} = 2,6\text{-}i\text{-Pr}_2\text{C}_6\text{H}_3$)

Raymond J. Butcher,^{1a} David L. Clark,^{*1b} Steven K. Grumbine,^{1c}
Rebecca L. Vincent-Hollis,^{1c} Brian L. Scott,^{1d} and John G. Watkin^{*1e}

Chemical Science and Technology (CST) Division, Los Alamos National Laboratory,
Los Alamos, New Mexico 87545

Received April 21, 1995[®]

Reaction of LaCl_3 with 3 equiv of sodium metal in liquid ammonia at -78°C , followed by addition of 3 equiv of HOAr ($\text{Ar} = 2,6\text{-}i\text{-Pr}_2\text{C}_6\text{H}_3$) in toluene produces $\text{La}(\text{OAr})_3(\text{NH}_3)_x$ (**1**) after warming to room temperature. Dissolution of **1** in toluene followed by 6 h reflux provides $\text{La}_2(\text{OAr})_6$ (**2**) in good yield. An X-ray crystallographic study revealed that **2** contains a dimeric unit held together with two η^6 -arene bridges formed from aryloxy ligands with $\text{La}-\text{C}(\text{av}) = 3.062(10)$ Å. The $\text{La}-\text{O}$ distances average 2.193(5) and 2.273(5) Å for terminal and bridging aryloxy ligands, respectively. Dissolution of **1** in toluene followed by vacuum filtration and crystallization from toluene without reflux yields $\text{La}_2(\text{OAr})_6(\text{NH}_3)_2$ (**3**) in high yield. The X-ray crystal structure of **3** reveals an alternate dimeric structure bridged by oxygen atoms of the aryloxy ligands. X-ray crystallography has shown that a third compound may be isolated by gravity filtration and crystallization of **1** to produce $\text{La}(\text{OAr})_3(\text{NH}_3)_4$ (**4**). **4** displays a capped pseudo-octahedral geometry around the metal center with facial aryloxy and NH_3 ligands. A fourth NH_3 ligand caps the face defined by the other three. $\text{La}-\text{O}$ distances for the aryloxy ligands average 2.252(6) Å. The $\text{La}-\text{N}$ distances for the NH_3 ligands average 2.750(9) Å with no significant lengthening of the capped $\text{La}-\text{N}$ bond. The monomeric five- and six-coordinate Lewis base adducts, $\text{La}(\text{OAr})_3(\text{THF})_2$ (**5**) and $\text{La}(\text{OAr})_3(\text{py})_3$ (**6**) ($\text{py} = \text{pyridine}$), are prepared by reaction of **2** with an excess of the appropriate Lewis base. An X-ray crystal structure for **5** displays a distorted trigonal bipyramidal La metal center with two axial THF and three equatorial aryloxy ligands. $\text{La}-\text{O}$ distances for aryloxy ligands average 2.21- (1) Å while $\text{La}-\text{O}$ distances for the THF ligands average 2.52(1) Å. Crystal data for **2** (-70°C): monoclinic space group $P2_1/c$, $a = 17.550(4)$ Å, $b = 10.225(2)$ Å, $c = 21.837(4)$ Å, $\beta = 111.57(3)^\circ$, $V = 3644.2$ Å³, $Z = 2$, $d_{\text{calc}} = 1.310$ g cm⁻³, $R(F) = 0.0394$, $R_w(F) = 0.0447$. Crystal data for **4** (-100°C): trigonal space group $R\bar{3}$, $a = 14.220(2)$ Å, $c = 32.821(4)$ Å, $V = 5748.8$ Å³, $Z = 6$, $d_{\text{calc}} = 1.259$ g cm⁻³, $R(F) = 0.0408$, $R_w(F) = 0.0497$. Crystal data for **5** (-70°C): monoclinic space group $P2_1$, $a = 9.870(2)$ Å, $b = 19.367(4)$ Å, $c = 12.128(2)$ Å, $\beta = 109.88(3)^\circ$, $V = 2180.1$ Å³, $Z = 2$, $d_{\text{calc}} = 1.241$ g cm⁻³, $R(F) = 0.0449$, $R_w(F) = 0.0583$.

Introduction

Alkoxide and aryloxy ligands have found an extensive use as ancillary ligands in inorganic chemistry due to their variable electron donation and π -buffering capabilities, their variable steric requirements, and the ability to bridge more than one metal center.^{2,3} Sattelberger *et al.* recently demonstrated that in 5f element chemistry, the 2,6-diisopropylphenoxide ligand could bridge between uranium centers in an unusual η^6 -bridging mode rather than a more conventional interaction with the oxygen atom of the ligand.⁴ In the solid state structure of $\text{U}_2(\text{OAr})_6$ ($\text{Ar} = 2,6\text{-}i\text{-Pr}_2\text{C}_6\text{H}_3$), the arene ring of an aryloxy ligand from one of the uranium metal centers coordinates to the second metal center through a multihapto interaction between the metal atom and the six carbon atoms of the arene ring.

We subsequently showed that 4f complexes of formula $\text{Ln}_2(\text{OAr})_6$ ($\text{Ln} = \text{Nd, Sm, Er}$) behave in a similar fashion.⁵ In that work, we postulated that the 2,6-diisopropylphenoxide ligand possessed unique steric requirements which were too demanding to bridge two metal atoms through the oxygen atom of the aryloxy ligand. In this report we describe our efforts to test this hypothesis by examining the synthesis of the corresponding $\text{Ln}_2(\text{OAr})_6$ analog for the largest lanthanide metal, *i.e.* lanthanum. This work has revealed additional factors influencing the coordination mode of the bridging 2,6-diisopropylphenoxide ligand in this system.

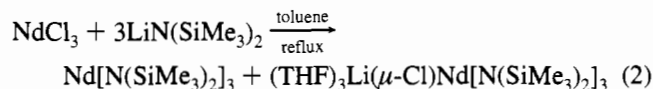
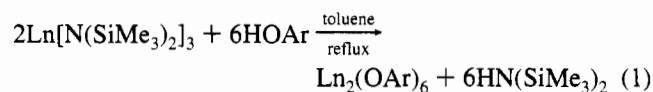
The general synthetic route reported previously for the preparation of $\text{Ln}_2(\text{OAr})_6$ complexes ($\text{Ln} = \text{Nd, Sm, Er}$) involves the alcoholysis of $\text{Ln}[\text{N}(\text{SiMe}_3)_2]_3$ with 2,6-diisopropylphenol in refluxing toluene solution (eq 1).⁵ For the lanthanide metals Nd, Sm and Er, the products can be isolated in good yields. Preparation of the lanthanum analog starting from $\text{La}[\text{N}(\text{SiMe}_3)_2]_3$ also produces $\text{La}_2(\text{OAr})_6$ according to the stoichiometry in eq 1, but the yields were variable and not consistent. We traced our difficulties with the yield of $\text{La}_2(\text{OAr})_6$ to problems associated with the synthesis of the silylamide precursor, $\text{La}[\text{N}(\text{SiMe}_3)_2]_3$, in a pure form and in high yield. It

[®] Abstract published in *Advance ACS Abstracts*, October 1, 1995.

- (1) (a) Current address: Department of Chemistry, Howard University, Washington, D. C. 20059. (b) CST-10, Mail Stop G739. (c) CST-10, Mail Stop C346. (d) CST-4, Mail Stop C345. (e) CST-18, Mail Stop C346.
- (2) Bradley, D. C.; Mehrotra, R. C.; Gaur, D. P. *Metal Alkoxides*; Academic Press: London, 1978.
- (3) Chisholm, M. H.; Rothwell, I. P. In *Comprehensive Coordination Chemistry*; Wilkinson, G.; Gillard, R.; McCleverty, J. A., Eds.; Pergamon Press: London, 1987; Vol. 2, p 335.
- (4) Van Der Sluys, W. G.; Burns, C. J.; Huffman, J. C.; Sattelberger, A. P. *J. Am. Chem. Soc.* **1988**, *110*, 5924.

- (5) Barnhart, D. M.; Clark, D. L.; Gordon, J. C.; Huffman, J. C.; Vincent, R. L.; Watkin, J. G.; Zwick, B. D. *Inorg. Chem.* **1994**, *33*, 3487.

is noteworthy that at least two modifications^{6,7} of the original preparation of $\text{La}[\text{N}(\text{SiMe}_3)_2]_3$ ^{8,9} have been reported in the last three years, suggesting that others have experienced similar difficulties in its preparation. Furthermore, we have encountered the carryover of alkali metal impurities in some subsequent reactions, the most striking example of which was the unanticipated isolation of the potassium salt complex $\text{K}[\text{La}(\text{OAr})_4]$ ^{10,11} from the reaction in eq 1, suggestive of a potassium impurity in $\text{La}[\text{N}(\text{SiMe}_3)_2]_3$ similar to the lithium impurity described by Edlmann and co-workers in the synthesis of $\text{Nd}[\text{N}(\text{SiMe}_3)_2]_3$ (eq 2).¹²



The alkali-metal salt problem pervades the literature in the field of f-element chemistry, and is an everpresent reality in metathetical reactions employing alkali metal ions. Similar problems have prompted many workers to perform extra synthetic steps in order to prepare iodide starting materials such as $\text{MI}_3(\text{THF})_4$ ($\text{M} = \text{Ln}, \text{An}$) prior to metathesis using potassium reagents.^{13,14} Obviously the search for improved starting materials is an attractive goal in this area.

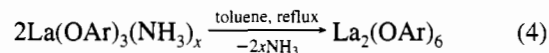
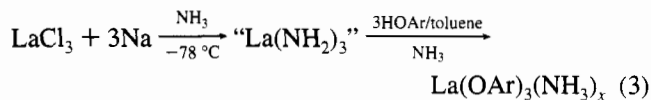
We have noted with great interest the resurgence of ammoniacal synthetic routes to prepare metal alkoxide complexes, which have been successfully employed in the synthesis of several uranium^{2,15-17} and alkaline earth¹⁸⁻²⁶ alkoxide complexes. We show in this report that an ammoniacal synthetic methodology circumvents many of the problems associated with the synthesis of $\text{La}[\text{N}(\text{SiMe}_3)_2]_3$ and $\text{La}_2(\text{OAr})_6$, and also that

- (6) Evans, W. J.; Golden, R. E.; Ziller, J. W. *Inorg. Chem.* **1991**, *30*, 4963.
 (7) LaDuca, R. L.; Wolczanski, P. T. *Inorg. Chem.* **1992**, *31*, 1311.
 (8) Bradley, D. C.; Ghotra, J. S.; Hart, F. A. *J. Chem. Soc., Chem. Commun.* **1972**, 349.
 (9) Bradley, D. C.; Ghotra, J. S.; Hart, F. A. *J. Chem. Soc., Dalton Trans.* **1973**, 1021.
 (10) Clark, D. L.; Gordon, J. C.; Huffman, J. C.; Vincent-Hollis, R. L.; Watkin, J. G.; Zwick, B. D. *Inorg. Chem.* **1994**, *33*, 5903.
 (11) Clark, D. L.; Huffman, J. C.; Watkin, J. G. *Inorg. Chem.* **1992**, *31*, 1554.
 (12) Edlmann, F. T.; Steiner, A.; Stalke, D.; Gilje, J. W.; Jagner, S.; Hakansson, M. *Polyhedron* **1994**, *13*, 539.
 (13) Avens, L. R.; Bott, S. G.; Clark, D. L.; Sattelberger, A. P.; Watkin, J. G.; Zwick, B. D. *Inorg. Chem.* **1994**, *33*, 2248.
 (14) Hazin, P. N.; Huffman, J. C.; Bruno, J. W. *Organometallics* **1987**, *6*, 23.
 (15) Jones, R. G.; Karmas, G.; Martin, G. A.; Gilman, H. *J. Am. Chem. Soc.* **1956**, *78*, 4285.
 (16) Cotton, F. A.; Marler, D. O.; Schwotzer, W. *Inorg. Chim. Acta* **1984**, *95*, 207.
 (17) Cotton, F. A.; Marler, D. O.; Schwotzer, W. *Inorg. Chem.* **1984**, *23*, 4211.
 (18) Drake, S. R.; Otway, D. J.; Hursthouse, M. B.; Abdul, M. K. M. *Polyhedron* **1992**, *11*, 1995.
 (19) Drake, S. R.; Streib, W. E.; Folting, K.; Chisholm, M. H.; Caulton, K. G. *Inorg. Chem.* **1992**, *31*, 3205.
 (20) Darr, J. A.; Drake, S. R.; Hursthouse, M. B.; Malik, K. M. A. *Inorg. Chem.* **1993**, *32*, 5704.
 (21) Darr, J. A.; Drake, S. R.; Williams, D. J.; Slawin, A. M. Z. *J. Chem. Soc., Chem. Commun.* **1993**, 866.
 (22) Drake, S. R.; Otway, D. J.; Perlepes, S. P. *Main Group Met. Chem.* **1991**, *14*, 243.
 (23) Drake, S. R.; Otway, D. J. *Polyhedron* **1992**, *11*, 745.
 (24) Drake, S. R.; Otway, D. J. *J. Chem. Soc., Chem. Commun.* **1991**, 517.
 (25) Caulton, K. G.; Chisholm, M. H.; Drake, S. R.; Folting, K. *Inorg. Chem.* **1991**, *30*, 1500.
 (26) Caulton, K. G.; Chisholm, M. H.; Drake, S. R.; Streib, W. E. *Angew. Chem. Int. Ed. Engl.* **1990**, *29*, 1483.

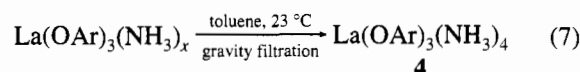
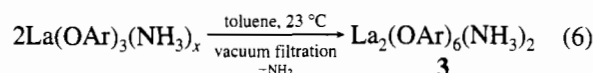
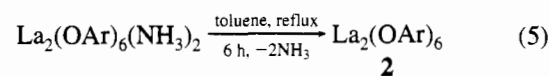
the small, volatile NH_3 ligand affords a method of reversible interconversion between the unusual η -arene and the more common oxygen-bridged dimeric structures.

Results and Discussion

Synthesis and Reactivity. Dissolution of LaCl_3 and 3 equiv of sodium metal in liquid ammonia at -78°C , followed by addition of 3 equiv of diisopropylphenol produces a white solid $\text{La}(\text{OAr})_3(\text{NH}_3)_x$ (**1**) after warming to room temperature as indicated in eq 3. We presume that the reaction proceeds *via*



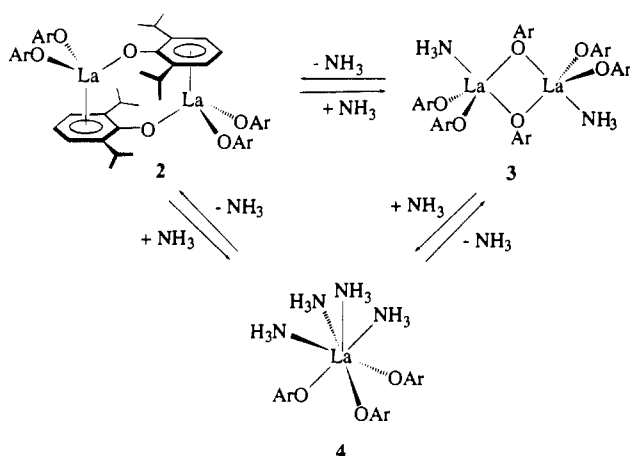
alcoholysis of the intermediate " $\text{La}(\text{NH}_2)_3$ ", but we have not attempted to isolate or characterize this product. Dissolution of **1** in toluene, followed by filtration and reflux for 6 h under a nitrogen atmosphere successfully removes all traces of ammonia. Low temperature crystallization from the toluene solution affords the desired dimeric product $\text{La}_2(\text{OAr})_6$ (**2**) as a white crystalline solid in a reproducible 50% yield according to eq 4. The reaction to generate **2** can also be conveniently carried out in a single step without first isolating **1**. Compound **2** is sparingly soluble in hexane and moderately soluble in benzene and toluene. Numerous attempts were made to characterize the initial ammonia adduct, $\text{La}(\text{OAr})_3(\text{NH}_3)_x$ (**1**). Due to the highly volatile nature of the NH_3 ligand, two different compounds could be reproducibly isolated which differ in the number of coordinated NH_3 ligands. When crude **1** (eq 3) is dissolved in toluene, vacuum filtered, and crystallized at low temperature, the monoammonia adduct $\text{La}_2(\text{OAr})_6(\text{NH}_3)_2$ (**3**) may be obtained in 80% yield according to eq 6. This compound is moderately soluble in benzene and toluene. The remaining NH_3 ligand is bound relatively strongly, and only upon prolonged (6 h) reflux in toluene can it be removed to form the base-free complex, **2** (eq 5).



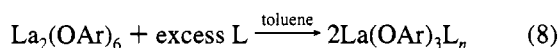
In contrast, if solid **1** is dissolved in toluene and gravity filtered, a different amine product (**4**) may be isolated which has only limited solubility in benzene and toluene. This product is extremely sensitive to ammonia loss to generate the dimeric monoammonia adduct **3**. The extreme difficulty in handling **4** without NH_3 loss made characterization extremely difficult. An X-ray diffraction study ultimately revealed one formulation of this material to be $\text{La}(\text{OAr})_3(\text{NH}_3)_4$ (**4**) (eq 7).

Other Lewis base adducts are conveniently prepared by dissolving crystalline $\text{La}_2(\text{OAr})_6$ (**2**) in a solution containing the respective Lewis base as indicated in eq 8. For example, addition of excess THF to **2** yields the bis-THF adduct, $\text{La}(\text{OAr})_3(\text{THF})_2$ (**5**) in a quantitative reaction as judged by ^1H

Scheme 1



NMR spectroscopy. Complex **5** can be isolated as clear, colorless crystals which are slightly soluble in hexane and moderately soluble in toluene and benzene. The tris(pyridine) adduct, $\text{La}(\text{OAr})_3(\text{py})_3$ (**6**), can be prepared from the reaction of excess pyridine with **2**. Compound **6** may be isolated in moderate yield as white, feathery needles which are slightly soluble in hexane and moderately soluble in benzene and toluene.



L = THF, $n = 2$; L = pyridine, $n = 3$; L = NH_3 , $n = 4$

With most Lewis bases such as THF or pyridine, the reaction in eq 8 is essentially irreversible. Any trace of THF or pyridine, even in the drybox atmosphere, will convert **2** into $\text{La}(\text{OAr})_3\text{L}_n$ compounds. ^1H NMR spectroscopy reveals that addition of NH_3 to solutions of $\text{La}_2(\text{OAr})_6$ (**2**) will generate $\text{La}_2(\text{OAr})_6(\text{NH}_3)_2$ (**3**). However, the extreme volatility of NH_3 gives a convenient method for removal of this ligand from solution, thereby forcing the reaction in eq 8 to the left, in favor of regenerating the base free **2**. This interconversion between complexes **2**, **3** and **4**, is outlined in Scheme 1. As indicated in the structural drawings of Scheme 1, the ammonia ligand has allowed for a facile interconversion between a traditional oxygen-bridged aryloxide dimer (**3**) and a nontraditional η -arene-bridged dimer (**2**) (*vide infra*).

Solid State and Molecular Structures. Four lanthanum complexes containing 2,6-diisopropylphenoxide ligation have been examined by single crystal X-ray diffraction techniques during the course of this work: $\text{La}_2(\text{O}-2,6-i\text{-Pr}_2\text{C}_6\text{H}_3)_6$ (**2**), $\text{La}_2(\text{O}-2,6-i\text{-Pr}_2\text{C}_6\text{H}_3)_6(\text{NH}_3)_2$ (**3**), $\text{La}(\text{O}-2,6-i\text{-Pr}_2\text{C}_6\text{H}_3)_3(\text{NH}_3)_4$ (**4**), and $\text{La}(\text{O}-2,6-i\text{-Pr}_2\text{C}_6\text{H}_3)_3(\text{THF})_2$ (**5**). The data for **3** were of poor quality, and could be refined to only 11%. Therefore, only the skeletal features of this structure will be discussed, and metrical data will not be presented. Data collection parameters for compounds **2**, **4**, and **5** are given in Table 1. Selected fractional coordinates for compounds **2**, **4**, and **5** are given in Tables 2–4, and selected bond lengths and angles are listed in Tables 5–7, respectively.

$\text{La}_2(\text{O}-2,6-i\text{-Pr}_2\text{C}_6\text{H}_3)_6$ (2**).** Single crystals of **2** suitable for an X-ray diffraction study were grown from a concentrated toluene solution at -40°C , and the structure was determined from diffraction data collected at -70°C . In the solid state, **2** displays a centrosymmetric, dimeric $\text{La}_2(\text{OAr})_6$ unit bridged by intermolecular η^6 - π -arene interactions of a unique aryloxide ligand as shown in Figure 1. In addition there is one unique toluene molecule per dimer within the lattice of **2**. The

Table 1. Summary of Crystal Data^a

	2	4	5
empirical formula	$\text{La}_2\text{C}_{79}\text{H}_{110}\text{O}_6$	$\text{LaC}_{36}\text{H}_{51}\text{N}_4\text{O}_3$	$\text{LaC}_{44}\text{H}_{67}\text{O}_5$
space group	$P2_1/c$	$R\bar{3}$	$P2_1$
cell dimens			
<i>a</i> , Å	17.550(4)	14.220(2)	9.870(2)
<i>b</i> , Å	10.225(2)		19.367(4)
<i>c</i> , Å	21.837(4)	32.821(4)	12.128(2)
β , deg	111.57(3)		109.88(3)
<i>T</i> , °C	-70	-100	-70
<i>Z</i> , mol/cell	2	6	2
<i>V</i> , Å ³	3644.2	5748.8	2180.1
<i>D</i> _{calc} , g cm ⁻³	1.310	1.259	1.241
$\lambda(\text{Mo K}\alpha)$, Å	0.710 73	0.710 73	0.710 73
fw	1433.56	738.83	814.93
abs coeff, cm ⁻¹	12.06	11.50	10.19
<i>R</i> (<i>F</i>) ^b	0.0394	0.0408	0.0449
<i>R</i> _w (<i>F</i>) ^c	0.0447	0.0497	0.0583

^a **2** = $\text{La}_2(\text{OAr})_6 \cdot \text{C}_7\text{H}_8$; **4** = $\text{La}(\text{OAr})_3(\text{NH}_3)_4$; **5** = $\text{La}(\text{OAr})_3(\text{THF})_2$ (Ar = 2,6-*i*-Pr₂C₆H₃). ^b $R(F) = \sum ||F_o| - |F_c|| / \sum |F_o|$. ^c $R_w(F) = [\sum w(|F_o| - |F_c|)^2 / \sum w|F_o|^2]^{1/2}$.

Table 2. Selected Atomic Coordinates and Equivalent Isotropic Displacement Coefficients^a (Å²) for $\text{La}_2(\text{O}-2,6-i\text{-Pr}_2\text{C}_6\text{H}_3)_6$ (**2**)

	10 ⁴ <i>x</i>	10 ⁴ <i>y</i>	10 ⁴ <i>z</i>	10 ³ <i>U</i> (eq)
La(1)	1508.0(3)	780.4(5)	932.6(2)	18.7(2)
O(2)	131(3)	987(5)	643(2)	20(2)
C(3)	-677(5)	848(8)	377(3)	22(3)
C(4)	-1056(5)	-266(7)	543(4)	19(3)
C(5)	-1904(5)	-381(7)	276(4)	21(3)
C(6)	-2389(5)	533(7)	-169(4)	26(3)
C(7)	-2020(5)	1598(8)	-343(4)	24(3)
C(8)	-1171(5)	1771(7)	-79(4)	22(3)
O(15)	2142(3)	-205(5)	1872(3)	23(2)
C(16)	2748(5)	-651(8)	2407(4)	22(3)
C(17)	2550(5)	-1375(8)	2890(4)	25(3)
C(18)	3184(5)	-1850(9)	3433(4)	35(4)
C(19)	3990(6)	-1648(10)	3522(5)	44(4)
C(20)	4180(5)	-923(9)	3061(4)	37(4)
C(21)	3567(5)	-425(7)	2501(4)	29(4)
O(28)	2125(3)	2673(5)	990(2)	25(2)
C(29)	2557(5)	3722(8)	1300(4)	22(3)
C(30)	2994(4)	4470(7)	1007(4)	20(3)
C(31)	3427(5)	5558(8)	1346(4)	31(4)
C(32)	3435(5)	5915(8)	1957(4)	33(4)
C(33)	3009(5)	5154(8)	2245(4)	29(4)
C(34)	2574(5)	4050(8)	1938(4)	26(3)
C(41)	5566(7)	11033(11)	111(5)	64(3)
C(42)	5723(7)	9958(13)	504(6)	72(3)
C(43)	5168(8)	8948(12)	409(6)	72(4)
C(44)	5290(14)	7729(25)	8000(11)	201(9)

^a Equivalent isotropic *U* defined as one-third of the trace of the orthogonalized U_{ij} tensor.

coordination geometry of each lanthanum atom approximates a three-legged piano stool. Each metal is bound to three terminal aryloxide oxygen atoms, and six carbon atoms of one of the aromatic rings of an aryloxide ligand bound to the symmetry-related metal atom in the dimeric unit (Figure 1). The overall structure is thus similar to that previously described for f-element diisopropylphenoxide dimers, $\text{M}_2(\text{OAr})_6$ where M = Nd,⁵ Sm,⁵ or U.⁴ The La–O bond lengths average 2.193(5) Å and 2.273(5) Å for terminal and bridging aryloxide ligands, respectively. The average terminal La–O distance of 2.193(5) Å may be compared with the average terminal La–O distances of 2.25(1), 2.253(6), 2.287(12), and 2.290(9) Å in $[\text{La}(\text{O}-2,6\text{-Ph}_2\text{C}_6\text{H}_3)_3(\text{THF})] \cdot \text{THF}$,²⁷ $\text{K}[\text{La}(\text{O}-2,6-i\text{-Pr}_2\text{C}_6\text{H}_3)_4]$,¹⁰ $\text{La}_2[\text{N}$ -

(27) Deacon, D. B.; Gatehouse, B. M.; Shen, Q.; Ward, G. N. *Polyhedron* **1993**, *12*, 1289.

Table 3. Selected Atomic Coordinates and Equivalent Isotropic Displacement Coefficients^a (Å²) for La(O-2,6-*i*-Pr₂C₆H₃)₃(NH₃)₄ (**4**)

	10 ⁴ x	10 ⁴ y	10 ⁴ z	10 ³ U(eq)
La(1)	3333*	6667*	3774(1)	18(1)
C(1)	155(5)	3561(5)	4090(2)	24(3)
C(2)	-493(6)	2543(5)	4243(2)	33(3)
C(3)	-57(6)	1996(5)	4444(2)	33(4)
C(4)	1058(6)	2489(6)	4502(2)	38(4)
C(5)	1749(5)	3526(5)	4364(2)	28(3)
C(6)	1292(5)	4087(5)	4155(2)	25(3)
O(1)	1939(3)	5099(3)	4014(1)	30(2)
N(1)	2038(6)	6930(6)	3217(2)	60(4)
N(2)	3330*	6660*	2909(10)	105(13)

^a Equivalent isotropic *U* defined as one-third of the trace of the orthogonalized *U*_{ij} tensor. Positions marked with an asterisk were not varied.

Table 4. Selected Atomic Coordinates and Equivalent Isotropic Displacement Coefficients^a (Å²) for La(O-2,6-*i*-Pr₂C₆H₃)₃(THF)₂ (**5**)

	10 ⁴ x	10 ⁴ y	10 ⁴ z	10 ³ U(eq)
La(1)	2218.8(4)	0*	7853.6(3)	25.3(1)
O(1)	1588(7)	620(4)	9154(6)	35(2)
O(2)	1373(7)	449(4)	6058(6)	38(3)
O(3)	3390(7)	-964(4)	8013(7)	41(3)
O(4)	102(8)	-709(4)	7798(7)	42(3)
O(5)	4649(7)	607(4)	8725(7)	43(3)
C(1)	557(11)	908(7)	5277(8)	40(4)
C(2)	-8780(13)	734(8)	4634(10)	51(5)
C(3)	-1722(13)	1234(10)	3881(10)	71(7)
C(4)	-1171(17)	1887(10)	3781(11)	70(6)
C(5)	200(15)	2036(8)	4419(11)	62(6)
C(6)	1107(12)	1555(6)	5177(8)	42(4)
C(13)	1051(9)	1009(5)	9848(7)	27(3)
C(14)	1162(9)	753(5)	10969(8)	32(3)
C(15)	586(11)	1168(6)	11651(9)	42(4)
C(16)	-111(12)	1758(7)	11231(11)	49(5)
C(17)	-205(11)	2005(6)	10135(10)	39(4)
C(18)	370(10)	1625(5)	9430(9)	34(3)
C(25)	4230(9)	-1512(5)	8084(8)	28(3)
C(26)	5043(11)	-1788(7)	9192(9)	41(4)
C(27)	5913(12)	-2334(7)	9236(12)	56(5)
C(28)	5983(11)	-2668(6)	8261(12)	50(5)
C(29)	5171(11)	-2400(6)	7157(11)	447(4)
C(30)	4296(9)	-1821(5)	7054(8)	31(3)
C(37)	-1077(13)	-560(7)	8207(13)	57(5)
C(38)	-1734(13)	-1219(7)	8307(12)	58(5)
C(39)	-1578(13)	-1632(7)	7285(11)	43(4)
C(40)	-100(14)	-1409(7)	7322(12)	52(5)
C(41)	4939(15)	1193(10)	9451(17)	92(8)
C(42)	6279(17)	1053(16)	10367(16)	143(13)
C(43)	7086(16)	545(13)	9844(15)	103(9)
C(44)	6016(11)	334(9)	8777(13)	71(6)

^a Equivalent isotropic *U* defined as one-third of the trace of the orthogonalized *U*_{ij} tensor. Positions marked with an asterisk were not varied.

(2,4,6-Me₃Ph)-salicylideneimato]₂(THF)₂(Cl)₂,²⁸ and [Me₄N][La₂-Na₂(O-4-MeC₆H₄)₉(THF)₅],²⁹ respectively, making this among the shortest La-O distance for an aryloxy ligand. The La-O-C bond angle for the bridging ligand is 165.4(5), and the La-O-C angles for the terminal ligands are 160.5(6) and 155.1(5).

Two η⁶-arene bridges bring the dimeric unit together with La-C distances of 3.062(10) Å (av) (range 2.978(10) - 3.164(9) Å). This distance is slightly greater than the average Ln-C distances of 3.035(12) (Nd) and 2.986(8) Å (Sm) seen for other Ln₂(OAr)₆ complexes,⁵ but is in accord with the somewhat larger

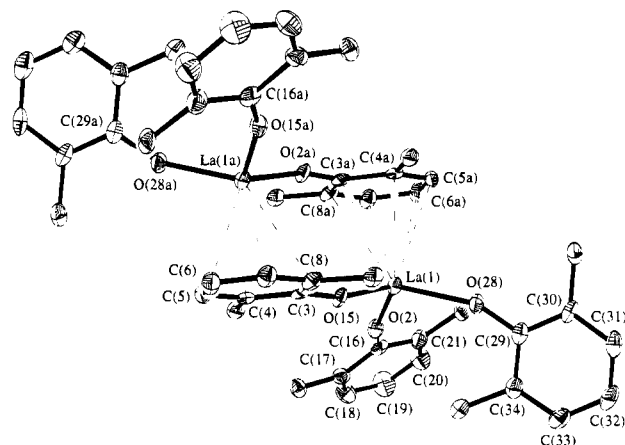


Figure 1. ORTEP plot (50% probability ellipsoids) showing the centrosymmetric η-arene-bridged dimeric structure of La₂(O-2,6-*i*-Pr₂C₆H₃)₆ (**2**) and giving the atom numbering scheme used in tables. Methyl carbon atoms of the isopropyl groups have been omitted for clarity.

Table 5. Selected Bond Distances (Å) and Angles (deg) for La₂(O-2,6-*i*-Pr₂C₆H₃)₆ (**2**)

La(1)-O(2)	2.273(5)	La(1)-O(15)	2.187(5)
La(1)-O(28)	2.198(5)	La(1)-C(3a)	3.164(9)
La(1)-C(4a)	3.067(7)	La(1)-C(5a)	2.995(9)
La(1)-C(6a)	2.978(10)	La(1)-C(7a)	3.038(9)
La(1)-C(8a)	3.133(8)		
O(2)-La(1)-O(15)	115.2(2)	O(2)-La(1)-O(28)	112.7(2)
O(15)-La(1)-O(28)	106.4(2)	La(1)-O(2)-C(3)	165.4(5)
La(1)-O(15)-C(16)	160.5(6)	La(1)-O(28)-C(29)	155.1(5)

Table 6. Selected Bond Distances (Å) and Angles (deg) for La(O-2,6-*i*-Pr₂C₆H₃)₃(NH₃)₄ (**4**)

La(1)-O(1)	2.259(4)	La(1)-N(1)	2.748(9)
		La(1)-N(2)	2.84(3)
La(1)-O(1)-C(6)	166.0(5)	O(1)-La(1)-O(1A)	108.5(1)
O(1)-La(1)-N(1)	92.9(2)	O(1)-La(1)-N(2)	110.3(1)
O(1)-La(1)-N(1a)	74.8(2)	O(1a)-La(1)-N(1)	155.4(2)
N(1)-La(1)-N(1A)	80.7(2)	N(1)-La(1)-N(2)	48.4(2)

Table 7. Selected Bond Distances (Å) and Angles (deg) for La(O-2,6-*i*-Pr₂C₆H₃)₃(THF)₂ (**5**)

La(1)-O(1)	2.233(8)	La(1)-O(4)	2.483(8)
La(1)-O(2)	2.227(7)	La(1)-O(5)	2.555(7)
La(1)-O(3)	2.169(7)		
La(1)-O(1)-C(13)	173.3(5)	La(1)-O(2)-C(1)	151.7(7)
La(1)-O(3)-C(25)	173.2(7)	O(1)-La(1)-O(2)	112.3(3)
O(1)-La(1)-O(3)	131.9(3)	O(2)-La(1)-O(3)	115.8(3)
O(1)-La(1)-O(4)	83.2(3)	O(1)-La(1)-O(5)	84.8(2)
O(2)-La(1)-O(4)	99.0(2)	O(2)-La(1)-O(5)	102.2(3)
O(3)-La(1)-O(4)	86.8(3)	O(3)-La(1)-O(5)	87.8(2)
O(4)-La(1)-O(5)	158.3(2)		

ionic radius of lanthanum. The La-C distance is also comparable to the Ln-C contacts observed in the other known examples of trivalent 4f element π-arene interactions, namely 2.89(3), 2.91(6), 2.93(3), 2.90(4), 2.999(23), 2.978(6), 3.04(6), and 3.08(2) Å observed in (η-C₆Me₆)Sm(AlCl₄)₃,³⁰ (η-C₆H₆)Sm(AlCl₄)₃,³¹ (η-C₆H₆)Nd(AlCl₄)₃,³¹ (η-1,3-Me₂C₆H₄)Sm(AlCl₄)₃,³¹ [(η-C₆Me₆)Eu(AlCl₄)₃]₄,³² Yb(O-2,6-Ph₂C₆H₃)₃,³³ Nd-

(28) Blech, P.; Floriani, C.; Chiesi-Villa, A.; Gustini, C. *J. Chem. Soc., Dalton Trans.* **1990**, 3557.

(29) Evans, W. J.; Golden, R. E.; Ziller, J. W. *Inorg. Chem.* **1993**, 32, 3041.

(30) Cotton, F. A.; Schwotzer, W. *J. Am. Chem. Soc.* **1986**, 108, 4657.

(31) Fan, B.; Shen, Q.; Lin, Y. *J. Organomet. Chem.* **1989**, 376, 61.

(32) Liang, H.; Shen, Q.; Jin, S.; Lin, Y. *J. Chem. Soc., Chem. Commun.* **1992**, 6, 480.

(33) Deacon, G. B.; Nickel, S.; MacKinnon, P.; Tiekink, E. R. T. *Aust. J. Chem.* **1990**, 43, 1245.

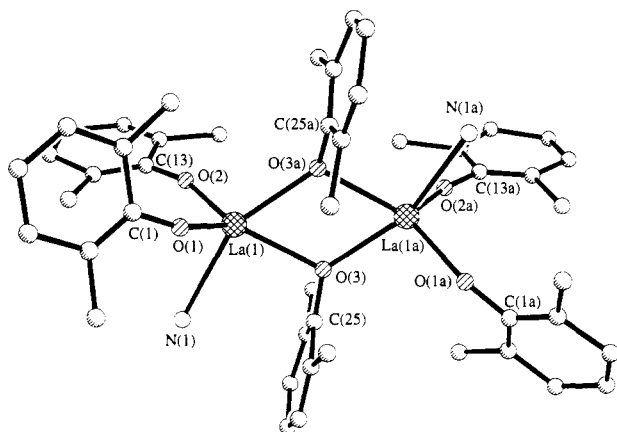


Figure 2. Ball-and-stick representation emphasizing the oxygen-bridged dimeric structure of $\text{La}_2(\text{O}-2,6-i\text{-Pr}_2\text{C}_6\text{H}_3)_6(\text{NH}_3)_2$ (**3**). Methyl carbon atoms of the isopropyl groups have been omitted for clarity.

($\text{O}-2,6\text{-Ph}_2\text{C}_6\text{H}_3$)₃,³⁴ and $\text{Nd}(\text{O}-2,6\text{-Ph}_2\text{C}_6\text{H}_3)_3(\text{THF})_3$,³⁴ respectively. These distances are, however, significantly longer than the Gd-C distance of 2.630(4) Å found for the zerovalent Gd- $(\eta\text{-}t\text{-Bu}_3\text{C}_6\text{H}_3)_2$.³⁵ The nonbonding La-La distance within the dimer is 5.595 Å.

$\text{La}_2(\text{O}-2,6-i\text{-Pr}_2\text{C}_6\text{H}_3)_6(\text{NH}_3)_2$ (3**).** Crystals of **3** suitable for an X-ray diffraction study were grown from a concentrated toluene solution at -40°C , and the structure was determined from diffraction data collected at -70°C . The structure refined to only 11%, and consequently bond distance and angle data are not included in this discussion. The structural data do unambiguously establish the connectivity of the atoms in **3**. In the solid state, **3** displays a centrosymmetric, dimeric $\text{La}_2(\text{OAr})_6(\text{NH}_3)_2$ unit containing a unique aryloxide ligand bridging through oxygen as shown in Figure 2. Each lanthanum atom adopts a distorted trigonal bipyramidal geometry, and the $\text{La}_2\text{O}_6\text{N}_2$ core can be viewed as two LaO_4N trigonal bipyramids joined along a common axial-equatorial edge. The fused trigonal bipyramidal geometry seen in **3** is similar to that observed in several other five-coordinate, dimeric f-element structures, including $[\text{Th}(\text{OCH}-i\text{-Pr}_2)_4]_2$,³⁶ and $[\text{U}(\text{NET}_2)_4]_2$.³⁷

$\text{La}(\text{O}-2,6-i\text{-Pr}_2\text{C}_6\text{H}_3)_3(\text{NH}_3)_4$ (4**).** Single crystals of **4** suitable for an X-ray diffraction study were grown from a concentrated toluene solution at -40°C , and the structure was determined from diffraction data collected at -100°C . In the solid state, **4** crystallizes in the trigonal space group $R\bar{3}$ with one NH_3 molecule in the lattice surrounded by three $\text{La}(\text{OAr})_3(\text{NH}_3)_4$ molecules. Each lanthanum atom displays a capped pseudooctahedral geometry of ligands with facial aryloxide and NH_3 ligands on a 3-fold axis. A fourth NH_3 ligand lies along the 3-fold axis and caps the face defined by the other three NH_3 ligands as shown in Figure 3. In addition there is some disorder associated with the capping NH_3 ligand resulting in a two-thirds occupancy of the capped position and a one-third occupancy as the NH_3 molecule within the lattice of **4**.

The La-O distances average 2.252(6) Å which is within the range of La-O distances observed previously (*vide supra*). The average O-La-O bond angle of 108.4° is slightly more obtuse than the expected 90° . This is particularly unusual for the

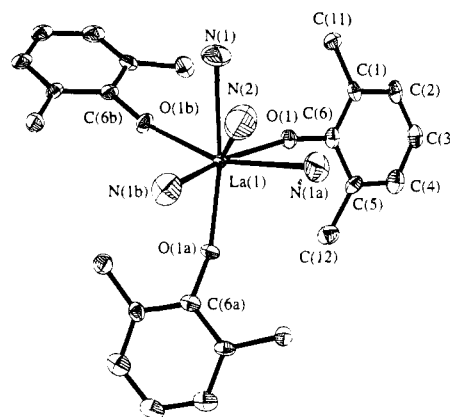


Figure 3. ORTEP representation (50% probability ellipsoids) of the capped octahedral coordination geometry of $\text{La}(\text{O}-2,6-i\text{-Pr}_2\text{C}_6\text{H}_3)_3(\text{NH}_3)_4$ (**4**), giving the atom numbering scheme used in the tables. Methyl carbon atoms of the isopropyl groups have been omitted for clarity.

noncapped face of a capped octahedral structure and may be attributed to the steric bulk of the disubstituted aryloxide ligands. This structure may be compared with several other capped octahedral structures including the hexagonal A-form of La_2O_3 , and $[\text{Y}(\text{C}_6\text{H}_5\text{COCHCOCH}_3)_3\cdot\text{H}_2\text{O}]$ which consist of LnO_7 coordination polyhedra.³⁸⁻⁴⁰ $\text{La}(\text{OAr})_3(\text{NH}_3)_4$ has an average La-N distance of 2.750(9) Å. The unique (capping) NH_3 ligand does not show a significant lengthening when compared to the other three NH_3 ligands. This distance lies in the range reported for La-N distances to nitrogen-containing Lewis bases which span 2.67-2.90 Å, and is slightly longer than the La-N distance of 2.70(1) reported for $(\eta\text{-C}_5\text{Me}_5)_2\text{LaNHMe}(\text{NH}_2\text{Me})$.⁴¹⁻⁴³ The La-N distance for **4** is also slightly longer than those found in other structurally characterized lanthanide ammonia complexes *i.e.* 2.69(1), 2.664(13), 2.55(3), 2.50(1), and 2.423(8) Å for $\text{Pr}_2\text{-}[\text{OCMe}(\text{CF}_3)_2]_6(\text{NH}_3)_4$,⁴⁴ $[(\eta\text{-C}_5\text{Me}_5)\text{Sm}]_4(\text{NHNH})_2(\text{NHNH}_2)_4(\text{NH}_3)_2$,⁴⁵ $(\eta\text{-C}_5\text{Me}_5)_2\text{Yb}(\text{TePh})(\text{NH}_3)$,⁴⁶ $(\eta\text{-C}_5\text{Me}_5)_2\text{Yb}(\text{THF})(\text{NH}_3)$,⁴⁷ and $(\eta\text{-C}_5\text{Me}_5)_2\text{Yb}(\text{SPh})(\text{NH}_3)$.⁴⁸ The N(1)-La-N(3) bond angles average $48.3(2)^\circ$, while the N(1)-La-O(1a) bond angle shows a slight decrease from the ideal 180° down to $155.5(2)^\circ$.

$\text{La}(\text{O}-2,6-i\text{-Pr}_2\text{C}_6\text{H}_3)_3(\text{THF})_2$ (5**).** Crystals of **5** suitable for an X-ray diffraction study were grown from a concentrated toluene solution at -40°C , and the structure was determined from diffraction data collected at -70°C . The complex crystallizes in the monoclinic space group $P2_1$ as discrete molecules with no unusual intermolecular contacts. The overall molecular structure in the solid state is isostructural to that previously reported for $\text{Ln}(\text{OAr})_3(\text{THF})_2$ complexes of Pr, Gd,

(34) Deacon, G. B.; Feng, T.; Skelton, B.; White, A. H. *Aust. J. Chem.* **1995**, *48*, 1.

(35) Brennan, J. G.; Cloke, F. G. N.; Sameh, A. A.; Zalkin, A. *J. Chem. Soc., Chem. Commun.* **1987**, 1668.

(36) Clark, D. L.; Huffman, J. C.; Watkin, J. G. *J. Chem. Soc., Chem. Commun.* **1992**, 267.

(37) Reynolds, J. G.; Zalkin, A.; Templeton, D. H.; Edelman, N. M.; Templeton, L. K. *Inorg. Chem.* **1976**, *15*, 2498.

(38) Cotton, F. A.; Legzdins, P. *Inorg. Chem.* **1968**, *7*, 1777.

(39) Pauling, L. *Z. Krist.* **1928**, *69*, 415.

(40) Sinha, S. In *Structure and Bonding*; Dunitz, J. D.; Hemmerich, P.; Holm, R. H.; Ibers, J. A.; Jørgensen, C. K.; Neilsands, J. B.; Reinen, D.; Williams, R. J. P., Eds.; Springer-Verlag: Berlin, 1975; Vol. 25, p 69.

(41) Gagne, M. R.; Stern, C. L.; Marks, T. J. *J. Am. Chem. Soc.* **1992**, *114*, 275.

(42) Smith, P. H.; Raymond, K. N. *Inorg. Chem.* **1985**, *24*, 3469.

(43) Smith, P. H.; Reyes, Z. E.; Lee, C.-W.; Raymond, K. N. *Inorg. Chem.* **1988**, *27*, 4154.

(44) Bradley, D. C.; Chudzynska, H.; Hammond, M. E.; Hursthouse, M. B.; Motevalli, M.; Wu, R. *Polyhedron* **1992**, *11*, 375.

(45) Wang, K.-G.; Stevens, E. D.; Nolan, S. P. *Organometallics* **1992**, *11*, 1011.

(46) Berg, D. J.; Andersen, R. A.; Zalkin, A. *Organometallics* **1988**, *7*, 1858.

(47) Wayda, A. L.; Dye, J. L.; Rogers, R. D. *Organometallics* **1984**, *3*, 1605.

(48) Zalkin, A.; Henley, T. J.; Andersen, R. A. *Acta Crystallogr.* **1987**, *43C*, 233.

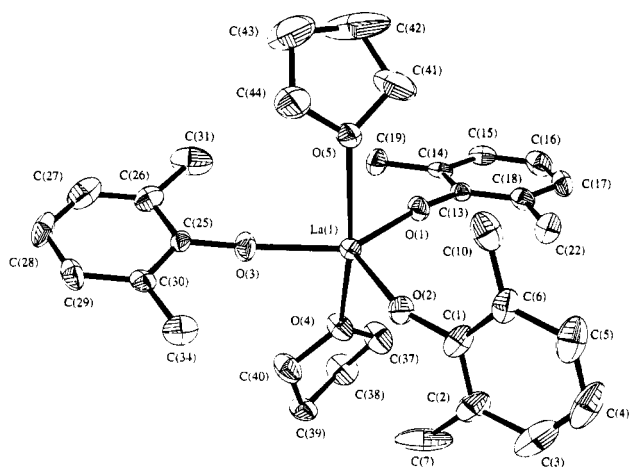


Figure 4. ORTEP drawing (50% probability ellipsoids) emphasizing the trigonal bipyramidal coordination geometry of $\text{La}(\text{O}-2,6\text{-}i\text{-Pr}_2\text{C}_6\text{H}_3)_3(\text{THF})_2$ (**5**) and giving the atom numbering scheme used in the tables. Methyl carbon atoms of the isopropyl groups have been omitted for clarity.

Er, and Lu which consist of distorted trigonal bipyramidal lanthanide metal centers with three equatorial aryloxy and two axial THF ligands as shown in Figure 4.⁵ Trigonal bipyramidal coordination has also been observed in $\text{Nd}(\text{OC}-t\text{-Bu})_3(\text{CH}_3\text{-CN})_2$,⁴⁹ $\text{Nd}(\text{O}-2,6\text{-Ph}_2\text{C}_6\text{H}_3)_3(\text{THF})_2 \cdot 2\text{THF}$,³⁴ and $\text{La}(\text{O}-2,6\text{-Ph}_2\text{C}_6\text{H}_3)_3(\text{THF})_2 \cdot \text{THF}$,²⁷ although the last complex features one axial and one equatorial THF ligand. The La–O distances for the aryloxy ligands average 2.21(1) Å which is as expected slightly longer than those for the analogous lanthanide complexes reported as 2.078 Å (Nd), 2.044 Å (Lu), 2.172 Å (Pr), and 2.130 Å (Gd), and within the range of La–O distances seen in **2** and **4**.

The La–O distances to the THF ligands average 2.52(1) Å and can be compared to 2.482(8) Å (Pr), 2.39(2) Å (Gd), 2.346–(2) Å (Er), and 2.296(2) Å (Lu) seen in related $\text{Ln}(\text{OAr})_3(\text{THF})_2$ structures.⁵ This value is identical to the La–O distance for the equatorial THF ligand in $\text{La}(\text{O}-2,6\text{-Ph}_2\text{C}_6\text{H}_3)_3(\text{THF})_2 \cdot \text{THF}$ although it is much shorter than the axial THF La–O distance of 2.68(2) Å in the same complex.²⁷ Additionally, **5** has relatively short La–O bond lengths for a THF ligand as compared with 2.54(2), 2.547(6), 2.56(1), and 2.642(8) Å found in $(\text{THF})_5\text{La}[(\eta\text{-C}_5\text{H}_5)\text{Mo}(\text{CO})_3]_3 \cdot \text{THF}$,⁵⁰ $\text{La}(\eta\text{-C}_5\text{Me}_5)[\text{CH}(\text{SiMe}_3)_2]_2(\text{THF})$,⁵¹ $[\text{La}(\text{BH}_4)_2 \cdot \text{THF}][\text{La}(\text{BH}_4)_4 \cdot \text{THF}]$,⁵² and $[\text{La}(\text{OSiPh}_3)_3(\text{THF})_3] \cdot \text{THF}$,⁵³ respectively.

A common feature seen in **5** and the related $\text{Ln}(\text{OAr})_3(\text{THF})_2$ structures is that two aryloxy ligands lie with their phenyl rings almost in the equatorial plane of the trigonal bipyramid, whereas the third aryloxy ligand (containing O(2)) is twisted noticeably out of this plane, presumably owing to the steric bulk of the diisopropylphenoxide ligands (Figure 4).⁵ The La–O–C angle of this unique aryloxy ligand is 151.7(7) vs 173.3(7)° (av) for the other two aryloxy ligands. The THF ligands bend away from this unique aryloxy ligand, resulting in an axial O–Ln–O angle between THF ligands of 158.3(2) which is

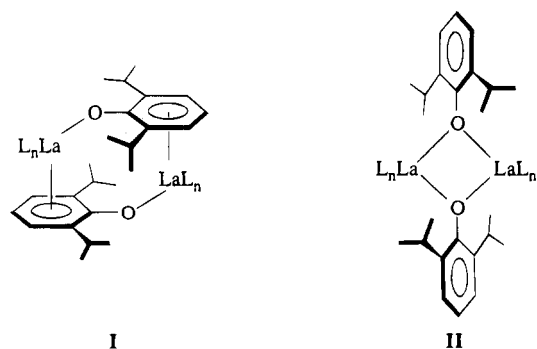
significantly smaller than the expected 180° angle for a trigonal bipyramidal molecule.

Spectroscopic Characterization. NMR Studies. The room temperature ¹H NMR spectra of the monomeric Lewis base adducts $\text{La}(\text{OAr})_3(\text{THF})_2$ (**5**) and $\text{La}(\text{OAr})_3(\text{py})_3$ (**6**) recorded in benzene-*d*₆ were consistent with expectations for monomeric complexes. The ¹H NMR spectrum of **5** shows one type of aryloxy and one type of THF ligand environment in a 3:2 ratio consistent with the formation of a bis-THF adduct. The ¹H NMR spectrum of **6** revealed one type of aryloxy and one type of pyridine ligand environment in a 1:1 ratio consistent with a tris(pyridine) adduct which adopts either a static *fac*-octahedral geometry in solution, or possesses a *mer* geometry with ligands rapidly equilibrating on the NMR timescale. A satisfactory ¹H NMR spectrum of the tetraammine adduct $\text{La}(\text{OAr})_3(\text{NH}_3)_4$ (**4**) could not be obtained due to rapid loss of ammonia to form the dimer $\text{La}_2(\text{OAr})_6(\text{NH}_3)_2$ (**3**). All attempts to record the spectrum of **4** revealed partial loss of ammonia resulting in integrations that were less than four ammine ligands per three aryloxy ligands. The ¹H NMR spectrum of **3** in benzene-*d*₆ reveals only one type of aryloxy and one type of amine ligand environment in a 3:1 ratio suggesting a fluxional process which equivalences the bridging and terminal ligands.

Ambient temperature ¹H NMR spectra of $\text{La}_2(\text{OAr})_6$ (**2**) in benzene-*d*₆ or toluene-*d*₈ solutions reveal two sets of somewhat broadened and slightly overlapping aryloxy resonances which integrate in an approximate 2:1 ratio. The broadening of the resonances appears to be due to the onset of bridge–terminal ligand exchange at room temperature, since spectra recorded at 0 °C show considerably sharper resonances. At –60 °C in toluene-*d*₈ the ¹H NMR spectrum of **2** clearly shows the presence of two distinct aryloxy ligand environments in a 2:1 ratio, suggesting that a dimeric structure is retained in solution as observed in the Nd, Sm, and Er analogs.⁵

At room temperature, ¹H NMR spectra of $\text{La}_2(\text{OAr})_6(\text{NH}_3)_2$ (**3**) show only one type of aryloxy ligand environment, together with a broad resonance assigned to the ammonia ligands, but at –60 °C in toluene-*d*₈ the spectrum clearly shows the presence of two distinct aryloxy ligand environments in a 2:1 ratio, indicating that the dimeric structure is retained in solution.

The similarities between the low temperature ¹H NMR spectra of the dimers **2** and **3**, despite their decidedly different bridging modes, suggested that NMR spectroscopy was not the best technique to determine the presence of oxygen- as opposed to η -arene-bridging aryloxy ligands in these dimeric species. Efforts were therefore turned to IR spectroscopy for more persuasive evidence to differentiate between possible bridging modes of the aryloxy ligands in $\text{La}_2(\text{OAr})_6$ and $\text{La}_2(\text{OAr})_6(\text{NH}_3)_2$ as indicated in **I** and **II**.



(49) Herrmann, W. A.; Anwander, R.; Kleine, M.; Scherer, W. *Chem. Ber.* **1992**, *125*, 1971.

(50) Pasynskii, A. A.; Eremenko, I. L.; Suleimanov, G. Z.; Nuriev, Y. A.; Beletskaya, I. P.; Shklover, V. E.; Struchkov, Y. T. *J. Organomet. Chem.* **1984**, *266*, 45.

(51) van der Heijden, H.; Schaverien, C. J.; Orpen, A. G. *Organometallics* **1989**, *8*, 255.

(52) Bel'skii, V. K.; Sobolev, A. N.; Bulychev, B. M.; Alikhanova, T. K.; Kurbonbekov, A.; Mirsaidov, U. *Koord. Khim.* **1990**, *16*, 1693.

(53) McGeary, M. J.; Coan, P. S.; Folting, K.; Streib, W. E.; Caulton, K. G. *Inorg. Chem.* **1991**, *30*, 1723.

Infrared Spectroscopic Studies. It has been shown previously that infrared spectroscopy provides invaluable information regarding the identification of η -arene-bridged dimeric structures

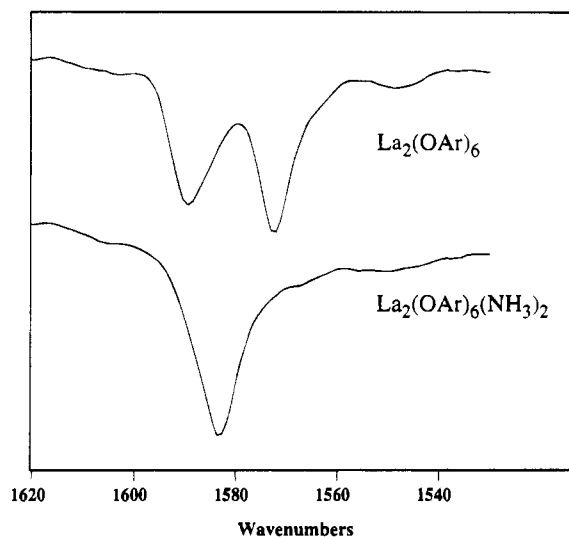


Figure 5. Comparison of the relevant $\nu(\text{C}=\text{C})$ stretching region of the solid-state IR spectra of η -arene-bridged $\text{La}_2(\text{OAr})_6$ (**2**) and oxygen-bridged $\text{La}_2(\text{OAr})_6(\text{NH}_3)_2$ (**3**) dimeric complexes.

Table 8. Infrared Vibration Frequencies (cm^{-1}) for the $\nu(\text{C}=\text{C})$ Stretch in Selected 2,6-Disubstituted Aryloxy Complexes^a

compound	$\nu(\text{C}=\text{C})$		medium	ref
	1	2		
$\text{La}_2(\text{OAr})_6$	1590	1572	Nujol	this work
$\text{La}_2(\text{OAr})_6$	1588	1572	benzene	this work
$\text{Nd}_2(\text{OAr})_6$	1588	1571	Nujol	5
$\text{Nd}_2(\text{OAr})_6$	1590	1572	benzene	5
$\text{Sm}_2(\text{OAr})_6$	1586	1572	Nujol	5
$\text{Sm}_2(\text{OAr})_6$	1589	1572	benzene	5
$\text{Er}_2(\text{OAr})_6$	1590	1571	Nujol	5
$\text{Er}_2(\text{OAr})_6$	1589	1572	benzene	5
$\text{U}_2(\text{OAr})_6$	1588	1553	Nujol	4
$\text{U}(\text{OAr})_3$	1583		Nujol	4
$\text{La}_2(\text{OAr})_6(\text{NH}_3)_2$	1583		Nujol	this work
$\text{KLa}(\text{OAr})_4$	1581		Nujol	10
$\text{La}(\text{OAr})_3(\text{THF})_2$	1587		Nujol	this work
$\text{Li}(\text{OAr})$	1584		Nujol	this work
HOAr	1585		neat	this work

^a Ar = 2,6-*i*-Pr₂C₆H₃; Ar' = 2,6-*t*-Bu₂C₆H₃.

for lanthanide and actinide metals.^{4,5} Infrared spectroscopy shows distinct differences in aromatic C=C vibrational modes for the π -bound and O-bridged aryloxy ligands in $\text{M}_2(\text{OAr})_6$ compounds. Indeed, the infrared spectra of $\text{La}_2(\text{OAr})_6$ show the presence of *two* distinct types of $\nu(\text{C}=\text{C})$ stretching modes in the aromatic region both in solution and in the solid state. The higher frequency band occurs at 1590 cm^{-1} in Nujol and at 1588 cm^{-1} in benzene solution, and is twice the intensity of the lower energy band. The second band appears at 1572 cm^{-1} in both the solid state and in solution. Two distinct C=C stretching modes were also seen in the solid state (Nujol mull) spectra of $\text{U}_2(\text{OAr})_6$ and in the solid state and solution spectra of the $\text{Ln}_2(\text{OAr})_6$ complexes that we previously reported.^{4,5}

Figure 5 compares the infrared spectra of the two dimers $\text{La}_2(\text{OAr})_6$ and $\text{La}_2(\text{OAr})_6(\text{NH}_3)_2$. $\text{La}_2(\text{OAr})_6(\text{NH}_3)_2$ shows only one type of aromatic C=C stretching mode as reported for the oxygen bridged dimer $\text{Y}_2(\text{O}-2,6\text{-Me}_2\text{C}_6\text{H}_3)_6(\text{THF})_2$.⁵⁴ Table 8 compares the $\nu(\text{C}=\text{C})$ stretching modes for La complexes prepared in this work, as well as several other relevant 2,6-diisopropylphenoxide complexes.^{4,5,10} $\text{La}_2(\text{OAr})_6(\text{NH}_3)_2$ (**3**), $\text{La}(\text{OAr})_3(\text{THF})_2$ (**5**), $\text{La}(\text{OAr})_3(\text{py})_3$ (**6**), LiOAr , and HOAr show a single $\nu(\text{C}=\text{C})$ stretch, which falls between 1590 and 1580

cm^{-1} . The presence of a second mode at 1572 cm^{-1} for $\text{La}_2(\text{OAr})_6$, as well as for the previously reported $\text{Ln}_2(\text{OAr})_6$ and $\text{U}_2(\text{OAr})_6$ dimers clearly indicates a weakening of the C=C bond, consistent with the π -arene interaction seen in the solid state structure. Perhaps most important is that the infrared spectrum of $\text{La}_2(\text{OAr})_6(\text{NH}_3)_2$ shows only a single $\nu(\text{C}=\text{C})$ vibrational mode consistent with an oxygen-bridged structure.

Concluding Remarks

The use of an ammoniacal route in the preparation of lanthanum aryloxy complexes has led to the convenient one-pot synthesis which avoids potential alkali metal contamination problems and low yields associated with the use of $\text{La}[\text{N}(\text{SiMe}_3)_2]_3$. We view this as a significant synthetic advance. This preparative methodology is convenient in its simplicity and suitability to scaleup.

The high volatility of the ammonia ligand allows a convenient method for ligand removal in the lanthanum aryloxy system, and the reversibility of Lewis base binding provides significant new insights into the nature of the La–OAr bonding in lanthanide 2,6-diisopropylphenoxide systems. We previously believed that the steric bulk of the 2,6-diisopropylphenoxide ligand was responsible for the formation of an η -arene bridge of the type $\text{La}_2(\mu\text{-}\eta^6\text{-OAr})_2(\text{OAr})_4$ (**I**) vs an oxygen bridge of the type $\text{La}_2(\mu\text{-OAr})_2(\text{OAr})_4$ (**II**). In light of the preparation of $\text{La}_2(\mu\text{-OAr})_2(\text{OAr})_4(\text{NH}_3)_2$ (**3**), which reveals an oxygen-bridging interaction, it seems clear that electronic factors are important in favoring one bonding mode over another in these aryloxy systems. Subtle changes in Lewis acidity at the metal center allow reversible changes in the bonding mode of the aryloxy ligand. In the absence of a Lewis base, the η -arene bridge is favored. Addition of a strong Lewis base such as ammonia results in a change in the aryloxy-bonding mode to the more common oxygen-bridge. This change in bonding is found to be reversible *via* the addition or removal of the volatile NH_3 ligand from the system.

Infrared spectroscopy has proven to be an invaluable technique in the identification of the η -arene-bridged (**I**) vs oxygen-bridged (**II**) dimeric structures, especially the presence of the distinctive lower energy aromatic C=C stretch at 1572 cm^{-1} in the spectrum of $\text{La}_2(\mu\text{-}\eta^6\text{-OAr})_2(\text{OAr})_4$ (**2**). This low frequency band appears to be a reliable indicator of an η -arene bridged structure, arising from the decrease in C=C bond strength upon coordination to a metal center. This feature is not observed in oxygen-bridged structures such as $\text{La}_2(\mu\text{-OAr})_2(\text{OAr})_4(\text{NH}_3)_2$ (**3**) or in monomeric complexes.

Experimental Section

General Procedures and Techniques. All manipulations were carried out under an inert atmosphere of oxygen-free UHP grade argon using standard Schlenk techniques or under oxygen-free helium in a Vacuum Atmospheres glovebox unless otherwise stated. Anhydrous lanthanum trichloride was purchased from Aldrich or Strem and used as received. 2,6-Diisopropylphenol was purchased from Aldrich and degassed before use. Potassium 2,6-diisopropylphenoxide was prepared from reaction of potassium hydride (Aldrich) with 2,6-diisopropylphenol in THF. KH was obtained as a 60% dispersion in mineral oil (Aldrich), washed with hexane, and vacuum dried. Sodium metal in mineral oil was purchased from Aldrich and washed with hexane prior to use. Anhydrous NH_3 was purchased from Matheson and used as received. $\text{La}[\text{N}(\text{SiMe}_3)_2]_3$ was prepared by refluxing lanthanum trichloride with 3 equiv of potassium bis(trimethylsilyl)amide in THF, followed by crystallization from hexane.^{6,7} Solvents were degassed and distilled from sodium benzophenone ketyl under nitrogen. Benzene-*d*₆ and toluene-*d*₈ were degassed, dried over Na–K alloy, and then trap-to-trap distilled before use. Solvents were taken into the glovebox and a small amount tested with a solution of sodium benzophenone ketyl in

(54) Evans, W. J.; Olofson, J. M.; Ziller, J. W. *Inorg. Chem.* **1989**, *28*, 4308.

THF. Solvents that failed to maintain a purple coloration from this test were not used.

NMR spectra were recorded at 22 °C on a Brüker WM300 spectrometer or at 15 °C on a Brüker AMX 500 spectrometer in benzene-*d*₆. All ¹H NMR chemical shifts are reported in ppm relative to the ¹H impurity in benzene-*d*₆ or toluene-*d*₈ set at δ 7.15 or 2.09, respectively. Infrared spectra were recorded on a Digilab FTS-40 spectrometer. Solid-state spectra were taken as Nujol mulls between KBr plates, while solution spectra were recorded in benzene solution vs a solvent blank in KBr cells. Elemental analyses were performed on a Perkin-Elmer 2400 CHN analyzer. Elemental analysis samples were prepared and sealed in tin capsules in the glovebox prior to combustion.

La₂(O-2,6-*i*-Pr₂C₆H₃)₆ (2). **Method A.** A 2.004 g (8.171 mmol) sample of LaCl₃ and 0.573 g (24.90 mmol) of Na were placed into a 250 mL Schlenk reaction vessel. The vessel was attached to a dry ice/acetone condenser and 150 mL of ammonia was condensed into the vessel. The blue solution was stirred at -78 °C for 30 min to allow complete dissolution of LaCl₃. Next, 4.368 g (24.50 mmol) of 2,6-diisopropylphenol dissolved in 50 mL of toluene was slowly added to the stirring solution. After 1 h the pale yellow reaction mixture was allowed to slowly warm to room temperature. Then, 1 h later, a vacuum was applied and the NH₃ was removed *in vacuo* for 16 h. The resulting white solid was dissolved into toluene (*ca.* 75 mL), filtered through Celite on a medium porosity frit, and placed in a 250 mL Schlenk reaction vessel. The vessel was attached to a reflux condenser, and the solution was refluxed for 6.5 h under nitrogen, before being returned to the drybox. The volatiles were removed *in vacuo*, and the resulting solid was washed once with hexane to remove excess phenol. The resulting material was dissolved in toluene and cooled to -40 °C for 12 h to yield clear colorless crystals. These crystals were found to powder upon prolonged exposure to vacuum. Yield: 2.987 g (54%).

Method B. A 1.05 g (1.69 mmol) sample of La[N(SiMe₃)₂]₃ was dissolved in 75 mL of toluene in a 250 mL Schlenk reaction vessel, and then 0.903 g (5.06 mmol) of 2,6-diisopropylphenol, dissolved in 10 mL of toluene, was added. The resulting solution was removed from the drybox and refluxed for 3 h. The solution was filtered through Celite, concentrated to 30 mL, and cooled to -40 °C. Overnight, a white crystalline solid was deposited. This solid was isolated by decantation and allowed to dry. A second crop of crystals was isolated by concentration of the filtrate and cooling again to -40 °C. Total yield: 0.510 g (45%). ¹H NMR (300 MHz, toluene-*d*₈, 293 K): δ 7.39 (br, 4 H, *meta* OAr), 7.04 (m, 10 H, overlapping *para* and *meta* OAr), 6.84 (t, *J* = 8 Hz, 4 H, *para* OAr), 3.37 (br, 12 H, CHMe₂), 1.27 (d, *J* = 7 Hz, 48 H, CHMe₂), 1.20 (br d, 24 H, CHMe₂). ¹H NMR (300 MHz, toluene-*d*₈, 213 K): δ 7.28 (d, *J* = 8 Hz, 4 H, *meta* OAr), 7.13 (d, 8 H, *meta* OAr), 6.96 (t, *J* = 8 Hz, 4 H, *para* OAr), 6.88 (t, *J* = 7 Hz, 2 H, *para* OAr), 3.42 (br m, 8 H, CHMe₂), 3.23 (br m, 4 H, CHMe₂), 1.33 (d, *J* = 6 Hz, 48 H, CHMe₂), 1.15 (d, *J* = 6 Hz, 24 H, CHMe₂). IR (Nujol, cm⁻¹): 1590 (m), 1572 (m), 1457 (s), 1431 (s), 1379 (m), 1354 (sh), 1324 (s), 1262 (s), 1250 (sh), 1202 (s), 1111 (m), 1096 (m), 1041 (m), 887 (s), 856 (s), 806 (m), 777 (m), 753 (s), 750 (sh), 692 (m), 580 (m), 566 (w), 552 (m). IR (Benzene, cm⁻¹): 1588 (w), 1572 (w), 1457 (m), 1426 (s), 1380 (w), 1368 (w), 1352 (m), 1326 (s), 1291 (w), 1263 (s), 1206 (m), 1140 (w), 1111 (w), 1096 (w), 933 (w), 885 (m), 854 (m), 803 (w), 793 (vw), 775 (w), 751 (m), 571 (w), 563 (vw), 551 (vw). Anal. Calcd for C₇₂H₁₀₂La₂O₆: C, 64.47; H, 7.66. Found: C, 63.63; H, 8.78.

La₂(O-2,6-*i*-Pr₂C₆H₃)₆(NH₃)₂ (3). A 5.015 g (20.45 mmol) sample of LaCl₃ and 1.417 g (61.63 mmol) of Na were placed into a 250 mL Schlenk reaction vessel. The vessel was attached to a dry ice/acetone condenser, and 100 mL of ammonia was condensed into the vessel. The resulting blue solution was stirred at -78 °C for 30 min to allow complete dissolution of LaCl₃. Next, 10.905 g (61.17 mmol) of 2,6-diisopropylphenol dissolved in 50 mL of toluene was slowly added to the stirring solution. After 1 h of stirring at -78 °C, the reaction was allowed to slowly warm for 3 h under an argon purge. The solution was then filtered through Celite on a medium porosity frit, and placed at -40 °C for 16 h to yield colorless crystals. Yield: 11.58 g (83%). ¹H NMR (300 MHz, toluene-*d*₈, 293 K): δ 6.95 (m, 12 H, *meta* OAr), 6.77 (m, 6 H, *para* OAr), 3.10 (br, 12 H, CHMe₂), 1.11 (br, 72 H, CHMe₂), 0.71 (br s, 6 H, NH₃). ¹H NMR (300 MHz, toluene-*d*₈, 213

K): δ 7.03 (d, *J* = 8 Hz, 8 H, *meta* OAr), 6.89 (t, *J* = 8 Hz, 4 H, *para* OAr), 6.81 (d, *J* = 7 Hz, 4 H, *meta* OAr), 6.76 (t, 2 H, *para* OAr), 3.58 (br, 4 H, CHMe₂), 3.05 (br, 8 H, CHMe₂), 1.20 (br d, *J* = 6 Hz, 24 H, CHMe₂), 1.10 (br, 48 H, CHMe₂), 0.35 (br s, 6 H, NH₃). IR (Nujol, cm⁻¹): 3365 (w), 3282 (w), 3054 (w), 1891 (w), 1880 (w), 1838 (w), 1795 (w), 1704 (w), 1693 (w), 1648 (w), 1583 (m), 1456 (s), 1424 (s), 1378 (s), 1365 (m), 1360 (w), 1335 (sh, w) 1331 (s), 1310 (sh, w), 1300(m), 1270 (s), 1211 (s), 1168 (s), 1139 (sh, m), 1113 (m), 1106 (m), 1092 (w), 1059 (w), 1043 (s), 958 (w), 949 (w), 943 (w), 930 (m), 899 (w), 883 (s), 854 (s), 803 (m), 794 (m), 755 (s), 723 (m), 685 (s), 612 (m), 594 (w), 564 (w), 547 (s), 469 (m), 431 (s), 410(s). Anal. Calcd for C₇₂H₁₀₈La₂N₂O₆: C, 62.87; H, 7.91; N, 2.04. Found: C, 61.94; H, 8.18; N, 2.16.

La(O-2,6-*i*-Pr₂C₆H₃)₃(NH₃)₄ (4). A 5.004 g (20.4 mmol) sample of LaCl₃ and 1.5 g (65 mmol) of Na were placed into a 250 mL Schlenk reaction vessel. The vessel was attached to a dry ice/acetone condenser and 150 mL of ammonia was condensed into the vessel. The solution was stirred at -78 °C for 30 min to allow complete dissolution of LaCl₃. Next, 10.92 g (61.25 mmol) of 2,6-diisopropylphenol dissolved in 50 mL of toluene was slowly added with stirring. After 1 h the reaction was allowed to slowly warm to room temperature. The resulting solution was gravity filtered through Celite on a medium porosity frit, and placed at -40 °C for 12 h yielding clear colorless crystals. This product is extremely sensitive to NH₃ loss. As a result, no microanalytical data were collected.

La(O-2,6-*i*-Pr₂C₆H₃)₃(THF)₂ (5). A 0.500 g (0.371 mmol) sample of La₂(OAr)₆ (2) was dissolved in 10 mL of THF. The solution was allowed to stir for 36 h and was then pumped to dryness. The solid was washed with hexane, filtered, and rapidly pumped to dryness again. This crude solid proved to be pure by ¹H NMR spectroscopy. Yield: 0.471 g (78%). ¹H NMR (300 MHz, benzene-*d*₆, 298 K): δ 7.15 (d, *J* = 7 Hz, 6 H, *meta* OAr), 6.87 (t, *J* = 7 Hz, 3 H, *para* OAr), 3.53 (septet, 6 H, CHMe₂), 3.47 (m, 8 H, α-THF), 1.31 (d, *J* = 7 Hz, 36 H, CHMe₂), 1.13 (m, 8 H, β-THF). IR (Nujol, cm⁻¹): 1587 (m), 1428 (s), 1407 (s), 1378 (s), 1357 (m), 1327 (s), 1264 (s), 1206 (s), 1177 (w), 1158(w), 1141(w), 1108 (m), 1097 (m), 1056 (m), 1042 (s), 1023 (s), 953 (w), 934 (m), 917 (w), 886 (s), 853 (s), 804 (m), 797 (w), 774 (m), 685 (s), 616 (w), 554 (s), 464 (w). Anal. Calcd for C₄₄H₆₅O₅La: C, 64.85; H, 8.29. Found: C, 65.19; H, 8.26.

La(O-2,6-*i*-Pr₂C₆H₃)₃(py)₃ (6). To a vigorously stirring solution of 0.301 g (0.224 mmol) of La₂(OAr)₆ (2) in 10 mL of toluene was added 0.178 g (2.25 mmol) of pyridine in 2 mL of toluene in a dropwise manner. The solution was allowed to stir for 5 min and was then cooled to -40 °C. Overnight, clear, colorless crystals were deposited. These were isolated by decantation and allowed to dry in the glovebox atmosphere. Yield: 0.209 g (53%). ¹H NMR (300 MHz, benzene-*d*₆, 298 K): δ 8.65 (m, 6 H, *ortho* py), 7.26 (m, 6 H, *J* = 7 Hz, *meta* OAr), 6.96 (t, *J* = 7 Hz, 3 H, *para* OAr), 6.77 (m, 3 H, *para* py), 6.40 (m, 6 H, *meta* py), 3.55 (septet, 6 H, *J* = 7 Hz, CHMe₂), 1.17 (d, *J* = 7 Hz, 36 H, CHMe₂). IR (Nujol, cm⁻¹): 1736 (w), 1732 (m), 1595 (m), 1585 (m), 1571 (m), 1485 (w), 1462 (s), 1377 (s), 1367 (m), 1330 (m), 1279 (w), 1264 (s), 1207 (s), 1152 (m), 1108 (w), 1095 (w), 1068 (w), 1060 (w), 1043 (w), 1035 (m), 1004 (w), 999 (m), 886 (m), 861-(w), 851 (s), 804 (w), 798(w), 766 (m), 751 (s), 722 (m), 707 (s), 705 (w), 686 (m), 619 (s), 595 (w), 572 (w), 549 (s). Anal. Calcd for C₅₁H₆₆LaN₃O₃: C, 67.46; H, 7.33; N, 4.63. Found (av): C, 67.88; H, 7.22; N, 4.51.

Crystallographic Studies. **La₂(O-2,6-*i*-Pr₂C₆H₃)₆ (2).** The colorless crystals were examined in mineral oil under an argon stream, and a suitable crystal measuring 0.25 × 0.18 × 0.10 mm was mounted on a glass fiber with silicone grease and transferred to the -70 °C nitrogen cold stream of an Enraf-Nonius CAD4 diffractometer. A total of 25 carefully-centered reflections were used to obtain a monoclinic unit cell, and data were collected in the 2θ range of 3 to 45°. Two reflections were chosen as intensity standards and were measured every 7200 s of X-ray exposure time, and two orientation controls were measured every 250 reflections.

The intensities were corrected for Lorentz and polarization effects, and an empirical absorption correction based on azimuthal scans was applied. The structure was readily solved by Patterson methods and subsequent difference Fourier maps. Anisotropic thermal parameters were included for all non-hydrogen atoms, excluding the solvent of

crystallization and the isopropyl methyl carbon atoms. After geometrical generation of hydrogen atoms which were constrained to "ride" upon the appropriate carbon atoms, final refinement using 3107 unique observed [$F > 4.0\sigma(F)$] reflections converged at $R = 0.0394$, $R_w = 0.0447$ {where $w = [\sigma^2(F) + 0.006(F)^2]^{-1}$ }. All calculations were performed using the SHELXTL PLUS suite of computer programs (Siemens Analytical X-ray Instruments, Inc, 1990).

La(O-2,6-*i*-Pr₂C₆H₃)₃(NH₃)₄ (4). An irregular shaped crystal was coated with a thin layer of mineral oil and epoxy and mounted on a thin glass fiber. The crystal was then immediately placed in a -100 °C N₂ stream on a Siemens P4/PC diffractometer. The lattice parameters were optimized from a least-squares calculation on 32 carefully centered reflections of high Bragg angle. Two check reflections monitored every 98 reflections showed a systematic degradation of intensities corresponding to 4–5% over the course of the data collection. All data reduction, including Lorentz and polarization corrections, structure solution and refinement, and graphics were performed using SHELXTL PC software. All data were corrected for absorption using an empirical method that assumed an ellipsoidally shaped crystal.

Systematic absences and statistics suggested the trigonal space group $R\bar{3}$. The structure was solved in this space group using Patterson techniques to reveal a La atom on a 3-fold axis. Subsequent Fourier synthesis revealed the C and O atom positions of the $-OAr$ groups and the N atom positions of the ammonia ligands. The geometry of the molecule was a *facial* pseudooctahedron, with the three ammonia ligands forming one face and the $-OAr$ ligands forming the other. However, this solution revealed two independent molecules per unit cell and failed to converge upon refinement. The $R\bar{3}$ solution was converted to $R\bar{3}$, resulting in only one independent molecule per unit cell. The structure converged in this space group to $R = 0.060$ with all non-hydrogen atoms being refined anisotropically. At this point a residual on the 3-fold axis of the molecule corresponding to a cap on the ammonia face of the octahedron was discovered. Also, a significant residual was noted on a 3-fold axis between molecules and surrounded by the isopropyl groups. These two peaks were modeled as ammonia molecules and the best refinement linked the site occupancy factors of these molecules together. This refinement resulted in a final $R = 0.041$ and site occupancy factors for the bound (N(2)) and lattice (N(3)) ammonia ligands of 0.620(7) and 0.380(7), respectively. It is postulated that the new crystals all contain complexes with four nitrogen atoms bound, but as the crystal ages it loses the capping ammonia molecule to the lattice and this accounts for the sof's of N(2) and N(3) being

tied together. This also explains the slow degradation of the crystal during the data collection. Such a mechanism is bound to degrade the quality of the crystal and probably accounts for $R(\text{int}) = 0.140$ observed during data merging. Hydrogen atoms were fixed on the $-OAr$ groups using the SHELXTL HFIX facility. The close proximity of the ammonia groups made hydrogen atom placement difficult; thus the hydrogen atoms on the ammonia ligands were ignored. The final refinement included anisotropic thermal parameters on all non-hydrogen atoms except for the lattice ammonia (N(3)).

La(O-2,6-*i*-Pr₂C₆H₃)₃(THF)₂ (5). The clear, colorless crystals were examined in mineral oil under an argon stream and a suitable crystal measuring $0.25 \times 0.28 \times 0.35$ mm was affixed to the end of a glass fiber using silicone grease. The crystal was then transferred to an Enraf-Nonius CAD4 diffractometer where it was cooled to -70 °C for characterization and data collection. A total of 25 carefully-centered reflections were used to obtain a monoclinic unit cell, and data were collected in the 2θ range of 3 to 45°. Two reflections were chosen as intensity standards and measured every 7200 s of X-ray exposure time, and two orientation controls were measured every 250 reflections. The intensities were corrected for Lorentz and polarization effects and an empirical absorption correction based on azimuthal scans was applied. The structure was readily solved by Patterson methods and subsequent difference Fourier maps. After inclusion of anisotropic thermal parameters for all non-hydrogen atoms and geometrical generation of hydrogen atoms which were constrained to "ride" upon the appropriate carbon atoms, final refinement using 3464 unique observed [$F > 4.0\sigma(F)$] reflections converged at $R = 0.0449$, $R_w = 0.0583$ {where $w = [\sigma^2(F) + 0.0009(F)^2]^{-1}$ }. All calculations were performed using the SHELXTL PLUS suite of computer programs (Siemens Analytical X-ray Instruments, Inc, 1990).

Acknowledgment. This work was performed under the auspices of the Laboratory Directed Research and Development Program. Los Alamos National Laboratory is operated by the University of California for the U.S. Department of Energy under Contract W-7405-ENG-36.

Supporting Information Available: Tables of crystal data, fractional coordinates and isotropic thermal parameters, bond distances, bond angles, and anisotropic thermal parameters for **2**, **4**, and **5** (15 pages). Ordering information is given on any current masthead page.

IC950487Q